Spectrochimica Acta Part A: Molecular and Biomolecular Spectroscopy 192 (2018) 59–66

Contents lists available at ScienceDirect

Spectrochimica Acta Part A: Molecular and Biomolecular Spectroscopy

journal homepage: www.elsevier.com/locate/saa

# A new silver metaniobate semiconductor of $Ag_{0.5}La_{0.5}Nb_2O_6$ with defect-perovskite structure

Longqing Mi [a], Yongyi Feng [a], Lei Cao [a], Mingqiang Xue [a], Yanlin Huang [a,*], Lin Qin [b], Hyo Jin Seo [b,*]

[a] State and Local Joint Engineering Laboratory for Novel Functional Polymeric Materials, College of Chemistry, Chemical Engineering and Materials Science, Soochow University, Suzhou 215123, China

[b] Department of Physics and Interdisciplinary Program of Biomedical, Mechanical & Electrical Engineering, Pukyong National University, Busan 608-737, Republic of Korea

ARTICLE INFO

*Article history:*
Received 30 March 2017
Received in revised form 27 October 2017
Accepted 1 November 2017
Available online 03 November 2017

*Keywords:*
Semiconductor
Photocatalysis
Niobate
Perovskite-type structure
Optical materials and properties
Luminescence

ABSTRACT

Silver-containing lanthanum metaniobate $Ag_{0.5}La_{0.5}Nb_2O_6$ nanoparticles were synthesized by sol-gel polymerized complex method. A typical defect-perovskite structure was confirmed by XRD Rietveld refinements. The surface characteristics of the sample were tested by SEM, TEM and EDS measurements. SEM and TEM show that the sample presents ball-like particles with the diameters of 100 nm to 400 nm. The sample shows both self-activated luminescence and photocatalytic activities. $Ag_{0.5}La_{0.5}Nb_2O_6$ has a direct transition with band energy of 2.85 eV. The Ag4d-O2p hybridization in the valence band contributes to the narrowed band gap. The luminescence properties of $Ag_{0.5}La_{0.5}Nb_2O_6$ have been investigated for the first time. The luminescence is characterized by two emission centers with maximum wavelength near 460 and 530 nm. The emission and excitation spectra, decay curves and the thermal quenching mechanism were discussed. $Ag_{0.5}La_{0.5}Nb_2O_6$ shows the efficient photocatalytic activities and the photodegradation rate for methylene blue dye (MB) can reach about 95% under visible light (>420 nm) irradiation in 5 h. The trapped experiments for the active species were tested and discussed, which verified that •OH radicals could be the major active species in photocatalysis.

© 2017 Elsevier B.V. All rights reserved.

## 1. Introduction

Usually the photo-induced electrons and hole (excitons) can be induced in a semiconductor after light excitation. The photo-induced electrons could have two basic fates inside the semiconductor particles; the first is the non-radiative transitions resulting in the heat by transferring energy to phonons, and the second one is a radiative transition of recombination with a hole creating a luminescence. Moreover, photocatalysis can happen on the surface of a semiconductor due to the interfacial redox reactions of holes and electrons under light excitation. Consequently, photocatalysis and luminescence have close relationship.

Some semiconductors could present both of them. For example, niobate-containing materials have been regarded as potential photocatalysts for water splitting and degradation of inorganic dyes [1]. Moreover, niobates have intrinsic luminescence due to the efficient charge transfer transitions (CT) from O-2p to vacant Nb-4d orbital in Nb—O groups. The optical transitions are essentially influenced by the lattice composition and its symmetry. The distortion and electronic properties of niobates can be greatly modified by some structural defects [2]. Meanwhile, energy can easily transfer from $NbO_6$ groups to other activator, e.g., the activator $Eu^{3+}$ or to the surface of particles [3]. In the latter case, photocatalysis could happen under the excitation of UV–visible light in a solution. Niobates have been reported to be one of the promising active photocatalysts such as $A_4Nb_6O_{17}$ (A = K and Rb) [4], $ZnNb_2O_6$ [5], $Sr_2Nb_2O_7$ [6], $Cs_2Nb_4O_{11}$ [7], $K_4Nb_6O_{17}$ and $KNb_3O_8$ [1].

Ag-containing compounds have been widely reported for the visible-light-driven photocatalysts. The Ag3d-O2p hybridization in valence band results in low band energy of photocatalysts [8–10]. Silver niobium as photocatalyst has been widely reported [11–13]. Meanwhile, it has been confirmed that niobates could show both photocatalysis and photoluminescence properties under UV–visible light excitation such as $Na_{0.6}Ag_{0.4}NbO_3$ [14], $Ag_{0.7}Na_{0.3}NbO_3$ [11], $ZnNb_2O_6$ [5], $Sr_2Nb_2O_7$ [6], $K_4Nb_6O_{17}$ [1].

In this work, $Ag_{0.5}La_{0.5}Nb_2O_6$ with defect-perovskite structure was firstly developed. This structure has a super-lattice cell with orthorhombic symmetry of space group *Pmmm*. The cation ions exceptionally occupy positions in the z = 0 plain of the lattice. Ag and La stoichiometrically occupy 1a positions in the lattices. The cation vacancies regularly distribute in the lattices at positions z = 1/2 [15]. 2D conductivity could take place [16]. Metaniobates have been reported for ion conductors with the possible applications as solid electrolytes or electrode materials in various electrochemical devices [15].

$Ag_{0.5}La_{0.5}Nb_2O_6$ nanoparticles were prepared via sol-gel method. The structural Rietveld refinement was conducted in a defect-

* Corresponding authors.
*E-mail addresses:* huang@suda.edu.cn (Y. Huang), hjseo@pknu.ac.kr (H.J. Seo).

https://doi.org/10.1016/j.saa.2017.11.006
1386-1425/© 2017 Elsevier B.V. All rights reserved.

perovskite structure. The band structure was reported. The Luminescence of the sample was characterized by the photoluminescence spectra, decay curves and thermal stability. Meanwhile, the photocatalytic activity was confirmed by the photodegradation on MB. The results are beneficial for further developing the optical materials in defect-perovskite niobates.

## 2. Experimental

$Ag_{0.5}La_{0.5}Nb_2O_6$ nanoparticles were synthesized via sol-gel polymerized complex method. The raw reactants are $La(NO_3)_3\cdot 6H_2O$ (99.99%, Aladdin), $AgNO_3$ (99.99%, Aladdin), and $NbCl_5$ (99.9%, Aladdin). Firstly, the starting material $NbCl_5$ was dissolved in methanol solution by adding a large excess of citric acid (CA, 99.5%, Sinopharm Chemical Reagent Co., Ltd) under continuous stirring until the complete dissolution of CA. After that, $AgNO_3$ and $La(NO_3)_3\cdot 6H_2O$ were added to the solutions. The mixtures were stirred to get a transparent solution and then ethylene glycols (EG) were added to the system. The solutions were heated at 150 °C to improve esterification of CA and EG resulting in a resin. The brown resins were heated at 400 °C for 2 h to obtain black solids. The powders were calcined at 800 °C for 3 h to get the final $Ag_{0.5}La_{0.5}Nb_2O_6$ products.

The phase formations were confirmed by X-ray powder diffraction (XRD) on a diffractometer (DRON-4-07) with a Cu Kα radiation (18 mA, 40 kV). The crystal structure was refined using Rietveld refinement by GSAS software. The optical absorption spectra were taken by UV–vis-NIR spectrophotometer (Cary 5000). X-ray photo-electron spectroscopy (XPS) measurements were finished on a VG Escalab 200 MKII spectrometer. The photoluminescence (PL) spectra were measured by a spectrometer (Perkin-Elmer LS-50B) and the excitation was a xenon discharge lamp.

The photocatalytic experiments were conducted by photo-degradation of MB solutions under visible light irradiation (λ > 420 nm). The photocatalytic reactions were finished in a quartz reactor. For a photocatalytic reaction, 0.1 g $Ag_{0.5}La_{0.5}Nb_2O_6$ powders were added in MB solutions (100 mL, 10 mg $L^{-1}$). After a sufficient equilibrium between desorption and adsorption in dark, the photocatalytic experiment was initiated. 3 mL solutions were taken from the reactor at the fixed time intervals, which were centrifuged to remove the particles. Then the optical absorption of the solutions containing MB was measured to evaluate the photocatalytic effects.

## 3. Result and Discussion

### 3.1. The Phase Formation

The phase formation, crystal structure and experimental unit cell parameters of $Ag_{0.5}La_{0.5}Nb_2O_6$ nanoparticles were confirmed via XRD Rietveld refinement by GSAS software. The refine model was based on $Li_{0.5}La_{0.5}Nb_2O_6$ (ICSD-99312) [17]. Fig. 1 is XRD refined pattern indexed on $Ag_{0.5}La_{0.5}Nb_2O_6$ with defect perovskite structure. No impurity phases were detected in XRD pattern. The obtained structure data and the atomic positions are given in Tables 1 and 2, respectively.

Fig. 2 shows the structure sketch of $Ag_{0.5}La_{0.5}Nb_2O_6$ along [001] modeled by the refined atomic coordinates in Table 2. The framework of $Ag_{0.5}La_{0.5}Nb_2O_6$ is constructed by corner-sharing $NbO_6$ octahedra. $Ag_{0.5}La_{0.5}Nb_2O_6$ nanoparticles crystallize in orthorhombic lattice with the space group of *Pmmm* (47). It is a characteristic defect perovskite with $NbO_6$ octahedra ordered in the lattices. $La^{3+}$ and $Ag^{+}$ ions randomly occupy the 12-coordination cation sites in the structure. The structure can be regarded to derive from $La_{2/3}\square_{4/3}Nb_2O_6$ (□ is vacancy in La site), 1a positions are fully occupied, and 1c positions (vacancies) are occupied. The bond angle of Nb—O—Nb in $NbO_6$ is close to 180 °C, which indicates the light-created charges can easily move in the framework [7].

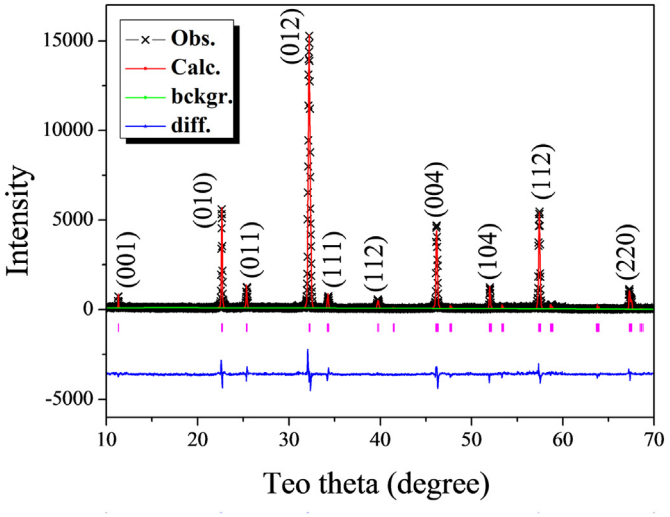


**Fig. 1.** The calculated (red line), measured (black cross), difference (bottom) of XRD Rietveld structure refinement of $Ag_{0.5}La_{0.5}Nb_2O_6$ photocatalyst. (For interpretation of the references to color in this figure legend, the reader is referred to the web version of this article.)

### 3.2. Morphology Characteristics

The typical morphological characteristic of $Ag_{0.5}La_{0.5}Nb_2O_6$ was tested by SEM measurements as displayed in Fig. 3(a, b, c). On the view from SEM micrographs with low-amplification, the sample shows loose aggregations, which can be easily separated or dispersed in solutions under a soft stir. The samples present ball-like particles with the diameters of 100 nm to 400 nm. EDS measurements were performed to detect the elements of the nanoparticles. Fig. 3(d) is the typical EDS measurements. It can be seen from it that the nanoparticles contain the elements of La, Ag, Nb and O. The detected ratio values of La/Ag and La/Nb are consistent with theoretical formula in $Ag_{0.5}La_{0.5}Nb_2O_6$ nanoparticles.

The TEM measurements of $Ag_{0.5}La_{0.5}Nb_2O_6$ nanoparticles are displayed in Fig. 4(a). The particles present the same profiles as those shown in SEM images. It presents the uniform ball-like particles with the diameters of 200 to 400 nm. Fig. 4(b) is the HRTEM image (high-resolution TEM) measured for $Ag_{0.5}La_{0.5}Nb_2O_6$ nanoparticles. The lattice fringe has an interplane distance about 0.278 nm corresponding to (012) lattice-space in the lattices. The selected area electron diffraction (SAED) selected in a single particle (Fig. 4c) can be indexed to

**Table 1**
The refined structure parameters of $Ag_{0.5}La_{0.5}Nb_2O_6$ at room temperatures.

| Formula | $Ag_{0.5}La_{0.5}Nb_2O_6$ |
|---|---|
| Radiation | Cu Kα |
| 2θ range(degree) | 10–120 |
| Symmetry | Orthorhombic |
| Space group# | *Pmmm* (47) |
| a/Å | 3.9338(4) |
| b/Å | 3.9395(3) |
| c/Å | 7.8566(6) |
| α/° | 90 |
| β/° | 90 |
| γ/° | 90 |
| Z | 2 |
| $R_p$ | 0.0962 |
| $R_{wp}$ | 0.1163 |
| $X^2$ | 21.93 |
| V | 121.76(3)Å$^3$ |

Download English Version:

https://daneshyari.com/en/article/7669633

Download Persian Version:

https://daneshyari.com/article/7669633

Daneshyari.com